

# Fourier-transform infrared and photoluminescence spectroscopies of self-assembled monolayers of long-chain thiols on (001) GaAs

Ximing Ding, Khalid Moumanis, and Jan J. Dubowski<sup>a)</sup>

Research Center for Nanofabrication and Nanocharacterization (CRN2), Université de Sherbrooke, Sherbrooke, Québec J1K 2R1, Canada

Lilin Tay

Institute for Microstructural Sciences, National Research Council of Canada, Ottawa, Ontario K1A 0R6, Canada

Nelson L. Rowell

Institute for National Measurement Standards, National Research Council of Canada, Ottawa, Ontario K1A 0R6, Canada

(Received 6 September 2005; accepted 26 January 2006; published online 10 March 2006)

Self-assembled monolayers (SAMs) of various thiols have shown the potential to protect freshly fabricated or chemically cleaned GaAs surfaces from oxidization, adsorption of foreign atoms, and/or surface defect formation. We have employed an attenuated total reflection Fourier-transform infrared spectroscopic technique to investigate the process of formation of long-chain thiols, comprising ten or more methylene chains, on the surface of (001) GaAs. A strong infrared (IR) signal was measured for all the investigated GaAs-thiol interfaces. Varying the type of terminal groups, from hydrophilic to hydrophobic, significantly changes the IR intensity of the methylene stretching vibration, indicating different methylene chain orientation in SAMs. Consequently, these SAMs exhibited different passivation performance to the (001) GaAs surface as judged by the intensity of the GaAs-related photoluminescence signal. © 2006 American Institute of Physics. [DOI: 10.1063/1.2178659]

## I. INTRODUCTION

Self-assembled monolayers (SAMs) formed on solid substrates such as alkylsiloxanes on SiO<sub>2</sub> (Ref. 1) and alkanethiols on Au and Ag (Ref. 2) have drawn substantial attention because of their potential to generate desired molecular architecture, to control the surface chemical and physical properties, and to provide capabilities for further chemical modification to immobilize functional moieties such as biomolecules and nanoparticles. Besides deposition on surfaces of coinage metals and oxides, SAMs of various thiols on III-V semiconductors have interested many researchers since Nakagawa reported octadecyl thiol SAMs on (001) GaAs.<sup>3-14</sup> Deposition of various thiols on GaAs and InP could lead to an enhanced photoluminescence (PL) signal from such materials as it has been reported by various authors.<sup>15,16</sup> The mechanism responsible for this behavior is likely related to the role that the thiol-provided sulfur plays in the passivation of exposed III-V surfaces.<sup>17</sup> No systematic study, however, has been available to demonstrate the role of the length of thiol's methylene chain (–CH<sub>2</sub>) and/or its terminal group on the intensity of the GaAs PL or on the passivation efficiency of this material.

Grazing angle incidence Fourier-transform infrared (GA-FTIR) spectroscopy has been established as one of the most sensitive surface analysis techniques to characterize SAMs on a plane metal surface.<sup>18-20</sup> It is able to probe the structure information of SAM patterns at a few tenths of a micrometer

of the lateral resolution.<sup>21</sup> A comparable GA-FTIR sensitivity and resolution have been demonstrated for SAMs of dioctadecyl disulfide (ODS) on gold and octadecyltrichlorosilane (OTS) on silicon surface.<sup>22</sup> This approach, however, is not widely applied for SAMs on nonmetallic substrates which have a low reflectivity and a striking influence of their optical properties on the SAM spectrum.<sup>23</sup> To obtain IR spectra of SAMs on GaAs, Baum *et al.* polished the edge of a GaAs crystal to a 45° trapezoidal geometry which provided approximately 36 internal reflections to the accumulative signal.<sup>11</sup> Obviously this approach does not suit high volume sample investigation.

Attenuated total reflection (ATR) FTIR spectroscopy is an alternative surface analysis technique, which is especially suitable for the investigation of thin films on low-reflecting nonmetallic substrates. For single reflection ATR-FTIR spectroscopy, a thin film is sandwiched between two high refractive index materials (the substrate and the prism), and the infrared light impinges the thin films at the critical angle<sup>24,25</sup> for the system. In this paper, we have employed ATR-FTIR to investigate the chain orientation of various thiols deposited on (001) GaAs. We have also carried out systematic PL measurements to investigate the influence of both the thiol chain length and the type of its terminal group on the passivation efficiency of the (001) GaAs surface.

## II. EXPERIMENTAL DETAILS

The five long-chain thiols that have been investigated with the ATR-FTIR and PL spectroscopies were 1-hexadecanethiol (HDT) (HS(CH<sub>2</sub>)<sub>15</sub>CH<sub>3</sub>), 16-

<sup>a)</sup>Author to whom correspondence should be addressed; electronic mail: jan.j.dubowski@usherbrooke.ca

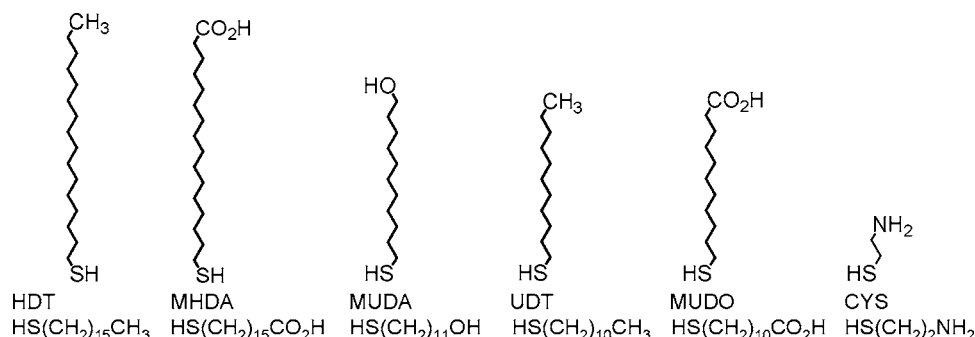


FIG. 1. Schematic diagram of the chemical structure of thiols investigated in this work: 1-hexadecanethiol (HDT), 16-mercaptohexadecanoic acid (MHDA), 11-mercaptoundecanoic acid (MUDA), 1-undecanethiol (UDT), 11-mercapto-1-undecanol (MUDO), and cysteamine (CYS).

mercaptohexadecanoic acid (MHDA) ( $\text{HS}(\text{CH}_2)_{15}\text{CO}_2\text{H}$ ), 1-undecanethiol (UDT) ( $\text{HS}(\text{CH}_2)_{10}\text{CH}_3$ ), 11-mercapto-1-undecanol (MUDO) ( $\text{HS}(\text{CH}_2)_{11}\text{OH}$ ), and 11-mercaptoundecanoic acid (MUDA) ( $\text{HS}(\text{CH}_2)_{10}\text{CO}_2\text{H}$ ). In addition, we carried out PL measurements for a sample coated with cysteamine (CYS) ( $\text{HS}(\text{CH}_2)_2\text{NH}_2$ ), which represents a case of a short-chain thiol. The chemical structure of the employed thiols is schematically shown in Fig. 1. The 15-methylene chain HDT and MHDA thiols are terminated either with hydrophobic ( $\text{CH}_3$ ) or hydrophilic ( $\text{CO}_2\text{H}$ ) groups. Similarly, two 10-methylene chain UDT and MUDA thiols are terminated either with  $\text{CH}_3$  or  $\text{CO}_2\text{H}$  groups. The 11-methylene chain MUDO thiol is terminated with a hydrophilic OH group. The 2-methylene chain CYS thiol is terminated with a hydrophilic  $\text{NH}_2$  group. The thiols were purchased from Aldrich and used as received.

The *p*-type (001) GaAs wafer (Zn doped,  $2 \times 10^{17}$  at.  $\text{cm}^{-3}$ , Sumitomo) was used for the deposition of the investigated thiols. Prior to SAM deposition, the wafer was cleaned in an ultrasonic bath sequentially with Opti-Clear, acetone and isopropanol for 5 min each (all solvents were VLSI grade). The wafer was then etched in concentrated HCl for 1 min and, subsequently, rinsed with deionized water. This etching gives a shiny and hydrophilic surface.

After drying in nitrogen flow, the wafer was immersed in a 5 mM thiol solution in ethanol and 5% aqueous ammonia. The SAMs investigated in this work were achieved following an 18-h immersion in the solution which was continu-

ously purged with nitrogen and heated to 55 °C. After SAM deposition, the wafer was rinsed with hot isopropanol, methanol, and water, and finally blown dried with nitrogen.

The ATR-FTIR spectra were collected with a Fourier transform spectrometer (model DA3, ABB Analytical Inc., Québec) for *p*-polarized radiation in the energy range of 600–6000  $\text{cm}^{-1}$ . The configuration of this measurement is shown in Fig. 2. The sample was brought into intimate contact with a Ge hemisphere attenuated total reflection prism. The mechanical pressure applied to the prism was monitored by employing a dial gauge. The measurements were carried out for the beam irradiating the prism at the angle near the critical for the Ge/GaAs interface ( $\sim 64^\circ$ ). The sample chamber was continuously purged with dry air. To avoid cross-contamination between different samples, the prism was cleaned by rinsing with organic solvents and etching in the oxygen plasma cleaner.

Low temperature PL spectra were measured at 20 K by irradiation of the SAM-covered and noncovered wafers with a 21 mW diode laser operating at 683 nm. A photomultiplier detector was employed to collect the PL signal. A simple washing and degreasing procedure of GaAs stored in an atmospheric environment for an extended period of time could result in an increase of the PL intensity by more than 200%.<sup>26</sup> Thus, the intensity of the PL signal observed in this work for all the investigated samples was always compared to that of a freshly degreased and etched GaAs sample. To

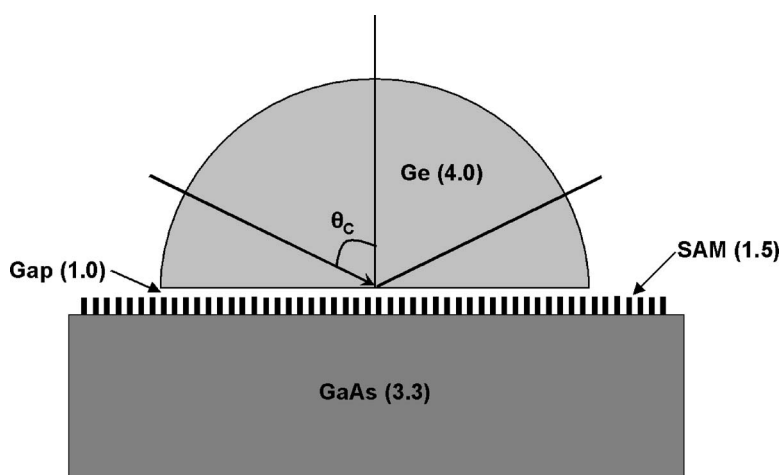


FIG. 2. Configuration of the attenuated total reflection measurements.

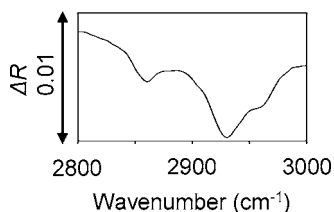


FIG. 3. ATR-FTIR spectroscopy of a (001) GaAs reference sample obtained with a freshly cleaned Ge prism.

minimize the influence of sample inhomogeneity, the spectra for each sample were measured at three positions and the results were averaged.

### III. RESULTS AND DISCUSSION

#### A. Prism cleaning and cross-contamination

Due to the close contact of the Ge prism with a sample, the presence of residual organics on the prism surface can lead to faulty signals. Any contaminants on samples could equally interfere with or even cover up the sample signal. Also, there is a very high risk that the contaminants will be transferred to following samples. Thus, the prism cleaning procedure should be considered as one of the critical issues in collecting the ATR-FTIR spectra. As an example, after measuring a protein sample, we observed a protein signature for the next few nonprotein samples if the prism was not properly cleaned. The best results were obtained if rinsing the prism with organic solvents was followed by cleaning with the oxygen plasma. Figure 3 shows a spectrum of a reference (001) GaAs wafer obtained with a freshly cleaned Ge prism. The  $\text{CH}_2$  (2855 and 2925  $\text{cm}^{-1}$ ) and  $\text{CH}_3$  (2960  $\text{cm}^{-1}$ ) signatures may result from the hydrocarbon contaminants in the dry air or the polymer layer coating the IR optics. The  $\text{CH}_2$  and  $\text{CH}_3$  signatures in the reference spectrum determine the detection limit of the thiol-related  $\text{CH}_2$  and  $\text{CH}_3$  signals obtained with the employed ATR-FTIR setup. Consequently, we considered that the positive identification of the presence of investigated SAMs could only take place if the amplitude of the  $\Delta R$  signal was greater than 0.005.

#### B. Spectroscopic analysis of thiol SAMs on (001) GaAs

Figures 4(a)–4(e) show the ATR-FTIR spectra of SAMs of HDT, UDT, MHDA, MUDA, and MUDO, respectively. The two peaks at  $\sim 2925$  and  $2855 \text{ cm}^{-1}$  which are assigned to asymmetric ( $\nu_{\text{as}}$ ) and symmetric ( $\nu_{\text{s}}$ )  $\text{CH}_2$  stretching vibrations indicate that the methylene chains are in *gauche* conformation for all investigated thiols. The highly organized thiol structure is expected to have asymmetric and symmetric vibrations at 2920 and 2850  $\text{cm}^{-1}$ , respectively.<sup>2</sup> The wide shoulder peak at 2965  $\text{cm}^{-1}$  corresponds to the asymmetric  $\text{CH}_3$  stretching vibration. The symmetric  $\text{CH}_3$  stretching vibration that usually appears at approximately 2880  $\text{cm}^{-1}$  has not been observed in this experiment. This suggests that the methyl group is out of the incident plane. The weak  $\text{CH}_3$  signatures at 2965  $\text{cm}^{-1}$  which have been seen in Figs.

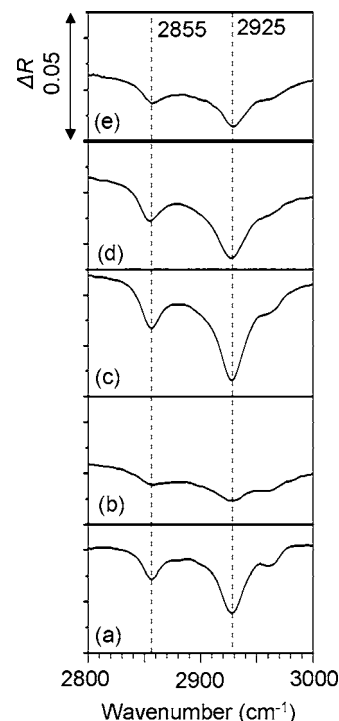


FIG. 4. ATR-FTIR spectroscopy of SAMs of various length chain thiols on (001) GaAs: (a)  $\text{GaAs-S(CH}_2\text{)}_{15}\text{CH}_3$ , (b)  $\text{GaAs-S(CH}_2\text{)}_{10}\text{CH}_3$ , (c)  $\text{GaAs-S(CH}_2\text{)}_{15}\text{CO}_2\text{H}$ , (d)  $\text{GaAs-S(CH}_2\text{)}_{10}\text{CO}_2\text{H}$ , and (e)  $\text{GaAs-S(CH}_2\text{)}_{11}\text{OH}$ .

4(c)–4(e) may originate from the background, as shown in Fig. 3.

The sensitivity of the ATR-FTIR technique strongly depends on the thickness of the air gap between the sample and the hemisphere prism,<sup>27,28</sup> which makes it quite challenging to make a quantitative analysis of the peak intensity. However, the results shown in Fig. 4 have been obtained nominally with the same pressure applied to the prism hemisphere, which makes it possible to carry out at least a semiquantitative analysis. For SAMs with the same number of  $-\text{CH}_2$  units, i.e., for Figs. 4(a) and 4(c) and for Figs. 4(b) and 4(d), the peak intensities of  $\nu_{\text{as}}$  and  $\nu_{\text{s}}$  are always higher when the thiols are terminated with hydrophilic groups of  $-\text{CO}_2\text{H}$  [Figs. 4(c) and 4(d)] than those terminated with hydrophobic  $-\text{CH}_3$  groups [Figs. 4(a) and 4(b)]. Though the methylene chains are in *gauche* conformation, they are expected to have a preferential average alignment. Thus, the observed results can be related to the methylene chain orientation. The strongest interaction of the electrical vector  $E$  of the incident light takes place when it is parallel to transition dipole moment  $V$ . This will result in the maximum IR signal. But, the weakest interaction and nearly zero signal are expected when  $E$  is perpendicular to  $V$ . It has been reported that the hydrophobic  $-\text{CH}_3$  terminated methylene chain is oriented at  $57^\circ$  to the GaAs (001) substrate normal.<sup>6</sup> When the incident beam impinges SAM at a critical angle, the evanescent wave propagates parallel to the prism-SAM interface and its electrical vector ( $E$ ) is perpendicular to the interface. For the symmetrical transition dipole moment  $V_{\text{s}}$ , which is perpendicular to the methylene axis, as shown in Fig. 5(a), the angle between  $E$  and  $V_{\text{s}}$  is  $33^\circ$ . Thus, the intensity of

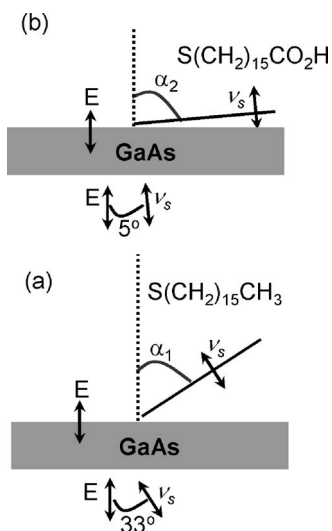


FIG. 5. Schematic diagram illustrating the strength of the interaction between the dipolar moment of symmetrical methylene stretching vibration ( $V_s$ ) and the electric field vector ( $E$ ) of the evanescent wave at the GaAs-thiol interface.

$-\text{CH}_2 v_s$  is proportional to  $V_s E \cos 33^\circ$ . The methylene chain with the hydrophilic terminal group will tilt towards the hydrophilic substrate with a bigger angle to the normal, as shown in Fig. 5(b) ( $\alpha_2 > \alpha_1$ ). For  $\alpha_2 \approx 85^\circ$ , the angle between  $E$  and  $V_s$  will be  $5^\circ$ , and the intensity of  $-\text{CH}_2 v_s$  will be proportional to  $V_s E \cos 5^\circ$ . Obviously the  $-\text{CO}_2\text{H}$  terminated methylene chain should have greater  $-\text{CH}_2 v_s$  and  $v_{\text{as}}$  intensities than those of the  $-\text{CH}_3$  terminated methylene chain.

This interpretation demonstrates the importance of terminal groups in dictating the orientation of methylene chains. When the terminal group is hydrophilic to the substrate, the methylene chains will be lying almost parallel to the substrate. When the terminal groups are hydrophobic to the substrate, the methylene chains tend to maintain a smaller tilted angle from the normal. For the five chemicals investigated in this report, we argue that the HDT and UDT form close-packed SAMs with methylene chains only weakly tilted from the (001) GaAs substrate normal. In contrast, MHDA, MUDD, and MUDA SAMs are less compacted and their methylene chains tend to be organized almost parallel to the substrate. The expected methylene chain orientations for the investigated thiols are illustrated in Fig. 6.

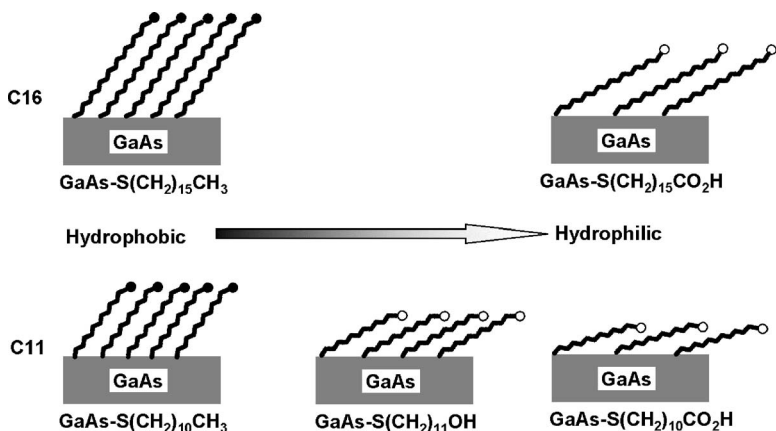


FIG. 6. Anticipated orientations of alkyl chains in SAMs of various thiols deposited on (001) GaAs.

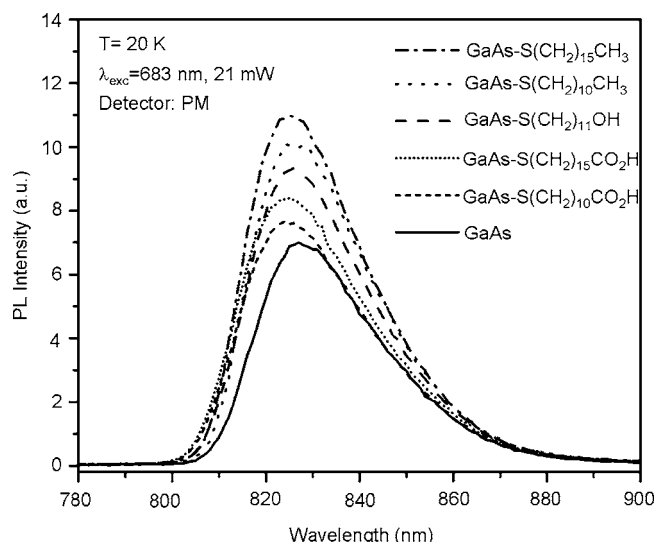


FIG. 7. Photoluminescence spectra of freshly etched (001) GaAs and samples covered with SAMs of different thiols.

### C. Photoluminescence spectra of (001) GaAs with thiol SAMs

The PL spectra from etched (001) GaAs and samples coated with SAMs of different thiols are shown in Fig. 7. The investigated peak ( $\lambda \approx 823$  nm) originates from the GaAs band gap emission. It can be seen that the PL signal from SAM coated samples clearly exceeds that from the etched only wafers. The PL enhancement, from the weakest of  $\sim 10\%$  to the strongest of  $\sim 50\%$ , follows the sequence of thiols from  $\text{S}(\text{CH}_2)_{10}\text{CO}_2\text{H}$ ,  $\text{S}(\text{CH}_2)_{15}\text{CO}_2\text{H}$ ,  $\text{S}(\text{CH}_2)_{11}\text{OH}$ , and  $\text{S}(\text{CH}_2)_{10}\text{CH}_3$  to  $\text{S}(\text{CH}_2)_{15}\text{CH}_3$ . The same result was also obtained for a different set of samples in our previous report.<sup>29</sup> In addition, when the PL signal was excited with an excimer laser operating at 248 nm, the same sequence of enhancement was observed with the strongest signal showing up to 2.5 times PL intensity enhancement.<sup>29</sup> The absorption coefficients of GaAs at 683 and 248 nm are  $1.8 \times 10^4$  and  $1.8 \times 10^6 \text{ cm}^{-1}$ , respectively.<sup>30</sup> This corresponds to the penetration depths of 550 and 5.5 nm, respectively. Thus, it is reasonable to expect that the greater amplitude of the enhancement observed with the shorter-wavelength laser is related to the more efficient probing of the near surface region of the sample.

For the same terminal group ( $\text{CH}_3$  or  $\text{CO}_2\text{H}$ ), the samples coated with SAMs of thiols having longer  $\text{CH}_2$  methylene chains have shown systematically greater amplitudes of the enhanced PL signal. Also, thiols with hydrophobic terminals ( $\text{CH}_3$ ) seemed to provide better passivation as judged by the more intense PL signal generated in samples coated with  $\text{S}(\text{CH}_2)_{15}\text{CH}_3$  and  $\text{S}(\text{CH}_2)_{10}\text{CH}_3$  in comparison to those coated with SAMs of  $\text{S}(\text{CH}_2)_{10}\text{CO}_2\text{H}$ ,  $\text{S}(\text{CH}_2)_{15}\text{CO}_2\text{H}$ , and  $\text{S}(\text{CH}_2)_{11}\text{OH}$ . The similar sequence of the enhancement observed for different sets of samples indicates that a reasonable reproducibility has been achieved in the surface preparation and deposition of SAMs of the investigated thiols. As shown in Fig. 6, the hydrophilic terminated SAMs provide a thinner passivation layer to the (001) GaAs and their passivation efficiency is limited due to their high affinity to ambient water and oxygen. But, the hydrophobic terminated SAMs, such as  $\text{GaAs-S}(\text{CH}_2)_{15}\text{CH}_3$  and  $\text{GaAs-S}(\text{CH}_2)_{10}\text{CH}_3$ , tend to be relatively highly organized and closely packed. They provide a higher concentration of sulfur atoms capable of neutralizing the greater concentration of nonradiative recombination centers at the surface of (001) GaAs. Such thiols are more effective in protecting the surface of GaAs from contacting ambient oxygen and moisture. Furthermore, longer-chain SAMs offer a thicker diffusion barrier, hence  $\text{GaAs-S}(\text{CH}_2)_{15}\text{CH}_3$  provided a significantly more stable interface when compared with  $\text{GaAs-S}(\text{CH}_2)_{10}\text{CH}_3$ . The superior stability of the (001) GaAs-thiol interface provided by the longer-chain SAMs of thiols and, especially, thiols with hydrophobic terminal groups has been confirmed by the x-ray photoelectron spectroscopy measurements.<sup>31</sup> In contrast, an investigation of the (001) GaAs surface coated with the short-chain CYS thiol had not shown a measurable enhancement of the PL signal. This result is in agreement with the results reported earlier, which had indicated the inability of the short-chain thiol to provide a robust interface with the gold substrate.<sup>2</sup>

The difference between the PL peak intensities for the same terminal group thiols, but having different length  $\text{CH}_2$  chains, has been systematically observed on different set of samples. This demonstrates that the applied method for the characterization of the GaAs-thiol interface is very sensitive to the physical and/or chemical properties of the interface that involves the investigated thiols. Clearly, the results indicate that the PL measurements can detect the difference (increased PL intensity) induced by the presence of five additional chains of  $\text{CH}_2$ . It is likely that this enhancement is due to the increased density of sulfur atoms afforded to the surface of GaAs by a more densely packed SAM with longer  $-\text{CH}_2$  chains aligned at a smaller angle to the surface normal than that with shorter chains. However, the exact and quantitative description of the mechanism of this enhancement requires a more extensive study.

#### IV. CONCLUSIONS

We have investigated SAMs of long-chain thiols on (001) GaAs with ATR-FTIR and PL measurements. The methylene chains are in *gauche* conformation and their preferred orientation is dictated by the terminal groups of thiols.

For a hydrophilic substrate, methylene chains with terminal hydrophobic groups are relatively highly ordered and closely packed as they tend to be organized with a small tilted angle to the substrate normal. In contrast, methylene chains of thiols with hydrophilic terminal groups incline to be organized almost parallel to the substrate. Consequently, they provided less efficient passivation of the investigated (001) GaAs surface as indicated by the modest enhancement of the PL signal. The lack of such an enhancement for a short-chain thiol terminated with the hydrophilic group ( $\text{HS}(\text{CH}_2)\text{NH}_2$ ) supports our conclusion concerning the role of the thiol methylene chain length in the successful formation of the stable thiol-GaAs interface. Long-chain thiols with the same length  $\text{CH}_2$  provided better passivation efficiency (higher PL signal enhancement) if their terminal groups were hydrophobic. For the same terminal groups ( $\text{CH}_3$  or  $\text{CO}_2\text{H}$ ), it has been determined that the 15- $\text{CH}_2$  chain thiols passivate the surface of (001) GaAs more efficiently than the 10- $\text{CH}_2$  chain thiols. Consistent with this observation is that HDT ( $\text{HS}(\text{CH}_2)_{15}\text{CH}_3$ ) SAM on (001) GaAs provided the most efficient passivation among all the thiols investigated in this work.

#### ACKNOWLEDGMENTS

The funding for this research has been provided by the Canadian Institutes for Health Research and the Canada Research Chair Program.

- <sup>1</sup>T. Vallant, H. Brunner, U. Mayer, H. Hoffman, T. Leitner, R. Resch, and G. Friedbacher, *J. Phys. Chem. B* **102**, 7190 (1998).
- <sup>2</sup>R. G. Nuzzo, L. H. Dubois, and D. L. Allara, *J. Am. Chem. Soc.* **112**, 558 (1990).
- <sup>3</sup>O. S. Nakagawa, S. Ashok, S. W. Sheen, J. Martensson, and D. L. Allara, *Jpn. J. Appl. Phys., Part 1* **30**, 3759 (1991).
- <sup>4</sup>S. R. Lunt, P. G. Santangelo, and N. S. Lewis, *J. Vac. Sci. Technol. B* **9**, 2333 (1991).
- <sup>5</sup>S. R. Lunt, G. N. Ryba, P. G. Santangelo, and N. S. Lewis, *J. Appl. Phys.* **70**, 7449 (1991).
- <sup>6</sup>C. W. Sheen, J. X. Shi, J. Maarensen, A. N. Parikh, and D. L. Allara, *J. Am. Chem. Soc.* **114**, 1514 (1992).
- <sup>7</sup>R. C. Tiberio, H. G. Craighead, M. Lercel, T. Lau, C. W. Sheen, and D. L. Allara, *Appl. Phys. Lett.* **62**, 476 (1993).
- <sup>8</sup>H. Ohno, M. Motomatsu, W. Mizutani, and H. Tokumoto, *Jpn. J. Appl. Phys., Part 1* **34**, 1381 (1995).
- <sup>9</sup>J. F. Dorsten, J. E. Maslar, and P. W. Bohn, *Appl. Phys. Lett.* **66**, 1755 (1995).
- <sup>10</sup>V. N. Bessolov, M. V. Lebedev, A. F. Ivankov, W. Bauhofer, and D. R. T. Zahn, *Appl. Surf. Sci.* **133**, 17 (1998).
- <sup>11</sup>T. Baum, S. Ye, and K. Uosaki, *Langmuir* **15**, 8577 (1999).
- <sup>12</sup>H. Ohno, L. A. Naghara, W. Mizutani, J. Takagi, and H. Tokumoto, *Jpn. J. Appl. Phys., Part 1* **38**, 180 (1999).
- <sup>13</sup>M. V. Lebedev, D. Ensling, R. Hunger, T. Mayer, and W. Jaegermann, *Appl. Surf. Sci.* **229**, 226 (2004).
- <sup>14</sup>V. L. Alperovich, O. E. Tereshchenko, N. S. Rudaya, D. V. Sheglov, A. V. Latyshev, and A. S. Terekhov, *Appl. Surf. Sci.* **235**, 249 (2004).
- <sup>15</sup>M. Schwartzman, V. Sidorov, D. Ritter, and Y. Paz, *Semicond. Sci. Technol.* **16**, L68 (2001).
- <sup>16</sup>T. Hou, C. M. Greenlief, S. M. Keller, L. Nelen, and J. F. Kauffman, *Chem. Mater.* **9**, 3181 (1997).
- <sup>17</sup>F. Seker, K. Meeker, T. F. Keuch, and A. B. Ellis, *Chem. Rev.* **100**, 2505 (2000).
- <sup>18</sup>H. C. Yang, D. L. Dermody, C. Xu, A. J. Rico, and R. M. Crooks, *Langmuir* **12**, 726 (1996).
- <sup>19</sup>P. Rowntree, *Surf. Sci.* **390**, 70 (1997).
- <sup>20</sup>E. Garand, J. F. Picard, and P. Rowntree, *J. Phys. Chem. B* **108**, 8182 (2004).

- <sup>21</sup>M. Hederos, P. Konradsson, and B. Lieberg, *Langmuir* **21**, 2971 (2005).
- <sup>22</sup>F. Bensebaa, P. L'Ecuyer, K. Faid, Ch. Py, T. J. Tague, and R. S. Jackson, *Appl. Surf. Sci.* **243**, 238 (2005).
- <sup>23</sup>H. Hoffmann, U. Mayer, H. Brunner, and A. Krischanitz, *Vib. Spectrosc.* **8**, 151 (1995).
- <sup>24</sup>J. A. Mielczarski, *J. Phys. Chem.* **97**, 2649 (1993).
- <sup>25</sup>J. E. Olsen and F. Shimura, *J. Appl. Phys.* **66**, 1353 (1989).
- <sup>26</sup>Kh. Moumanis, X. Ding, and J. J. Dubowski (unpublished).
- <sup>27</sup>T. Lummerstorfer and H. Hoffmann, *Langmuir* **20**, 6542 (2004).
- <sup>28</sup>N. Rochat, A. Chabli, F. Bertin, M. Olivier, C. Vergnaud, and P. Mur, *J. Appl. Phys.* **91**, 5029 (2002).
- <sup>29</sup>X. Ding and J. J. Dubowski, *Proc. SPIE* **5713**, 545 (2005).
- <sup>30</sup>A. Dargys and J. Kundrotas, *Handbook on Physical Properties of Ge, Si, GaAs and InP* (Science and Encyclopaedia, Vilnius, Lithuania, 1994).
- <sup>31</sup>D. Wieliczka, X. Ding, and J. J. Dubowski (unpublished).